

Resonant processes involving the production of three charged particles

M. Yu. Kuchiev and S. A. Sheinerman

A. F. Ioffe Physicotechnical Institute, Academy of Sciences of the USSR, Leningrad

(Submitted 5 November 1985)

Zh. Eksp. Teor. Fiz. **90**, 1680–1689 (May 1986)

Inelastic collisions $X + Y \rightarrow A + D$ are considered for arbitrary atoms X, Y in which the particle D is in a quasistationary state and decays via $D \rightarrow B + C$ to give three charged particles A, B , and C in the final state. The influence of their Coulomb interaction on the reaction cross section is considered, and a simple analytic solution is derived for a wide range of particle velocities. The “postcollision” interaction of A, B , and C in the final state greatly alters the angular distribution and energy spectrum. The results are compared with available experimental data, and experimental techniques for observing the predicted effects are discussed.

I. INTRODUCTION

In this paper we examine inelastic collisions between arbitrary atoms X and Y in which two other atoms A and D are produced, where D is in a quasistationary state and decays $D \rightarrow B + C$ to give three particles A, B , and C in the final state. We thus consider reactions of the type



where X, Y, A, B, C , and D are arbitrary atomic particles. We will assume that A, B, C , and D are charged and analyze how the Coulomb interaction between A, B, C in the final state affects the reaction cross section. We will see that the cross section for reaction (1) is greatly altered, and qualitatively new effects occur.

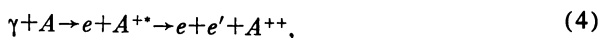
Among the processes (1) actively studied in recent years, we may mention the excitation of autoionizing atomic states by ion-atom collisions¹:



or electron impact:



photoionization of the inner atomic shells:



is another example. In all these reactions the autoionizing atomic state gives rise to a final state with three charged particles.

The consequences of the particle interaction in the final state (the postcollision interaction, or PCI) have been studied theoretically¹⁻⁹ for the case when the autoionizing electron in (2)–(4) moves so rapidly that its interaction with the other two particles is negligible. This situation occurs near the excitation threshold for the autoionizing state, and in this case only the interaction between two particles in the final state is important [between the ions I and A^+ in (2), or between a slow electron e and ions A^+, A^{++} in (3) and (4)]. Various models—classical,¹ shake-down,²⁻³ semiclassical,⁴ quasimolecular-adiabatic,⁵ quantum-mechanical,⁶⁻⁸ refined semiclassical⁹—have been used to analyze PCI; al-

though the details differ, these models all lead to similar results.

The case when the two final-state electrons in reactions (3), (4) have comparable energies was recently considered in Ref. 10 by using a simple physical model which indicated that the interaction among all three particles in the final state plays an important role. The same conclusion was reached in Ref. 11, where the classical equations for two electrons moving in the field of an ion were solved numerically.

In the present paper we show that the Coulomb interaction of the three particles in reaction (1) can be treated exactly for a wide range of particle velocities in the final state, and the problem admits an analytic solution. This is because all three particles interact only if the distance between them is large. The results are valid even for slowly moving particles in the final state, when perturbation theory is inapplicable.

The quasistationary nature of the intermediate state D in (1) gives rise to a line in the energy spectrum for the particles A, B , and C . If the latter do not interact, the line is Lorentzian with width equal to the full width Γ of the state D . In what follows we will analyze the spectra of the particles A, B, C near the resonance line. Other coherent but nonresonant processes can be neglected, because their cross sections vary smoothly.

We will see that the three-particle interaction in the final state greatly distorts the Lorentzian lineshape; the line becomes broader and asymmetric, and the maximum intensity decreases and is shifted. All these spectral changes are extremely sensitive to the scattering angles of the particles, which determine even the direction of the spectral shift and the sign of the asymmetry parameter.

This paper is organized as follows. In Sec. 2 we qualitatively describe the processes that occur in the final state of reaction (1). Expressions for the amplitude and cross section for (1) are derived in Sec. 3, while Sec. 4 applies the results to some particular reactions of the type (2)–(4), compares the results with available experimental data, and discusses how the predicted effects might be confirmed experimentally. We employ atomic units $|e| = \hbar = m_e = 1$ throughout this paper.

2. THE IMPORTANCE OF LARGE DISTANCES. EIKONAL APPROXIMATION

The width of the quasistationary intermediate state D in the atomic reactions (2)–(4) is usually small ($\Gamma < 1 \text{ eV} \approx 1/27 \text{ a.u.}$) and may thus be regarded as a small parameter. The distance between particles A and D at the instant of decay $D \rightarrow B + C$ is given approximately by $r_{AD} \approx V_{AD}/\Gamma$. We will assume that r_{AD} is large,

$$r_{AD} \approx V_{AD}/\Gamma = R \gg 1 \quad (5)$$

and write $r_{ij} = |\mathbf{r}_i - \mathbf{r}_j|$ and $V_{ij} = |\mathbf{V}_i - \mathbf{V}_j|$, where \mathbf{r}_i and \mathbf{V}_i are the position vector and velocity of particle i , $i = A, B, C, D$.

The distance r_{BC} between particle B and C may be large, small, or intermediate. For small $r_{BC} \ll R$, B and C interact strongly; however, this interaction can be treated using the ordinary two-body model. According to (5), the distance from particle A to the pair $B + C$ is large, so that its Coulomb interaction with $B + C$ is essentially the same as the interaction of A with D , which again is a two-body problem.

The situation changes only if the distance between B and C is considerable, $r_{BC} \approx R$, in which case we have a three-body problem. We conclude by combining the condition $r_{BC} \approx R$ with (5) that a full-fledged three-body problem arises only for configurations in which all three particles are well-separated:

$$r_{AB} \approx r_{AC} \approx r_{BC} \approx R. \quad (6)$$

However, the problem then simplifies considerably for the following three reasons. 1) The internal structure of A, B, C , their form-factors, polarizabilities, etc., may be neglected when treating the Coulomb interaction. 2) The three-body quantum-mechanical problem for the motion of the particles becomes semiclassical. 3) The Coulomb potential energy of the interacting particles is a small quantity. We will henceforth assume that it is much less than the kinetic energy; more precisely, we assume that

$$|Z_A Z_B|/r_{AB} \ll \varepsilon_{AB}, \quad |Z_A Z_C|/r_{AC} \ll \varepsilon_{AC}. \quad (7)$$

Here Z_i is the charge of particle i and $\varepsilon_{ij} = m_i m_j (m_i + m_j)^{-1} V_{ij}^2/2$ is the kinetic energy of particles i and j in their center-of-mass system. Inequalities (7) are assumed valid along all classical trajectories lying within the region (6); they imply that the particles A, B , and C move uniformly along straight-line classical trajectories.

The semiclassical equations for quasi-uniform motion along straight trajectories has a simple solution given by the eikonal approximation. Here we should mention that the eikonal approximation is usually employed to describe the motion of fast particles, whereas in our case it is not necessary to assume large relative particle velocities. Indeed, the inequalities (5) and (7) underlying our treatment may hold even for velocities < 1 because the width Γ is assumed to be small.

We also observe that the trajectories will actually be approximated by straight lines only in the large-separation region (6); the decay process $D \rightarrow B + C$ and the initial por-

tion of the trajectory of the pair $B + C$ will be described quantum mechanically, as will the motion of the pair $A + D$ for small distances r_{AD} .

Conditions (7) constrain the energies and scattering angles of the particles, but there are any processes (2)–(4) for which they are satisfied. For example, unless the scattering angle of the photo- and Auger electrons is very small ($\theta < 5^\circ$), (7) holds for photoelectron energies $E_A \gtrsim \Gamma^{2/3}$.

It is thus necessary to treat a full three-body interaction only for large distances (5)–(7). We will see that the exact solution of this problem leads to some qualitatively new results.

3. AMPLITUDE AND CROSS SECTIONS FOR THREE-PARTICLE PRODUCTION

We expand the amplitude as an infinite series of Feynman diagrams; some of the lowest-order diagrams are shown in Fig. 1. The straight lines describe the propagation of the particles X, Y, A, B, C, D , while the wavy lines describe the Coulomb interaction. The vertices (circles) describe the inelastic collision $X + Y \rightarrow A + D$ and the decay $D \rightarrow B + C$. We use the standard correspondence rules¹² to evaluate the diagrams and exploit the fact that Γ is small (Sec. 2). We will see that each diagram can be evaluated in the eikonal approximation, after which the total amplitude follows by adding all the diagrams. This approach was developed previously^{13,14} to handle problems when the long-range interaction among charged particles is important.

The simple diagram in Fig. 1a gives the contribution

$$A_0 = \frac{M_1 M_2}{-\varepsilon + i\Gamma/2} = -i M_1 M_2 \int_0^\infty \exp\{i(-\varepsilon + i\Gamma/2)t\} dt \quad (8)$$

to the amplitude, where M_1 is the matrix element for the inelastic scattering $X + Y \rightarrow A + D$, M_2 is the matrix element for the decay $D \rightarrow B + C$, and

$$\varepsilon = E_A + E_B - E_X - E_Y, \quad (9)$$

where E_i is the sum of the internal and kinetic energies of particle i . The second equality in (8) corresponds to passing

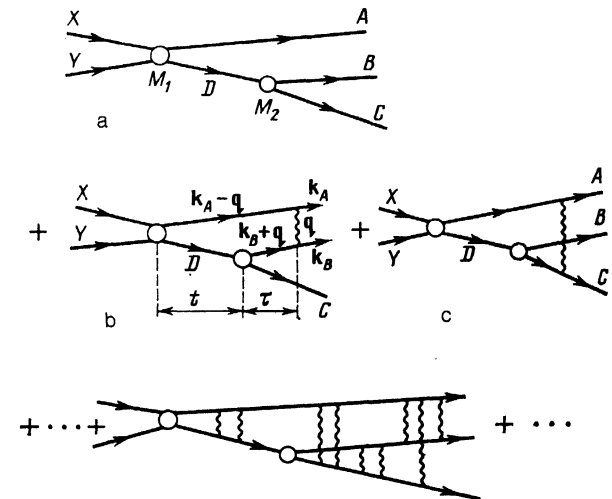


FIG. 1. Diagrams for three-particle interaction in the final state for resonant collisions (1).

to the time representation, which is convenient when adding the higher-order perturbation-theoretic diagrams.^{13,14} The variable t is interpreted as the lifetime of particle D .

We next evaluate the diagram in Fig. 1b, which describes the interaction between particles A and B in the final state to lowest order perturbation theory. Its contribution to the amplitude is

$$A_1 = \int \frac{M_1(\mathbf{k}_A - \mathbf{q}) M_2(\mathbf{k}_B + \mathbf{q})}{(-\varepsilon + E_A - E_{k_{A-q}} + i\Gamma/2)(E_A + E_B - E_{k_{A-q}} - E_{k_{B+q}} + i0)} \times \frac{4\pi Z_A Z_B}{q^2} \frac{d\mathbf{q}}{(2\pi)^3}. \quad (10)$$

Here \mathbf{k}_A and \mathbf{k}_B are the momenta of A and B in the final state, and $4\pi Z_A Z_B / q^2$ is the Fourier component of the Coulomb potential. Since we consider a resonant process, ε is small, $|\varepsilon| \sim \Gamma$. Small momentum transfers q

$$q \ll \Gamma / V_A, \quad q \ll k_A, k_B, \quad (11)$$

therefore give the dominant contribution to the integral (10). Since we assume that Γ is small, $\Gamma \ll m_A V_A^2 / 2$, $m_B V_B^2 / 2$, the first inequality in (11) implies the second. According to (6) and (7), small q corresponds to large r_{AB} . We can use (11) to simplify the integral (10) by retaining only the terms linear q in the energy denominators; in addition, the matrix elements M_1 and M_2 in (10) are assumed to vary slowly with \mathbf{q} and can be treated as constants in the integration. With these simplifications, the diagram in Fig. 1(b) can be evaluated in the eikonal approximation.¹⁵ Passing to the time representation, we find the simple expression

$$A_1 = (-i)^2 M_1 M_2 \int_0^\infty dt d\tau \exp\{i(-\varepsilon + i\Gamma/2)t\} U_1(t, \tau), \quad (12)$$

for the amplitude, where

$$U_1(t, \tau) = Z_A Z_B / |\mathbf{V}_{AD}(t+\tau) - \mathbf{V}_B \tau|. \quad (13)$$

As in (8), the variable t in (12) is interpreted as the lifetime of particle D ; τ is the time after the decay $D \rightarrow B + C$, as shown schematically in Fig. 1b.

The first-order diagram for the $A-C$ interaction (Fig. 1c) and the other higher-order diagrams can be evaluated similarly. In all cases the principal contribution comes from small momentum transfers q in the $A-B$ and $A-C$ interactions, and simplification yields an expression similar to (12) for the diagram in Fig. 1b. Summation then gives the expression

$$A = -i \tilde{M}_1 \tilde{M}_2 \int_0^\infty dt \exp\left\{(-\varepsilon + i\Gamma/2)t - \int_0^t U(t, \tau) d\tau\right\} \quad (14)$$

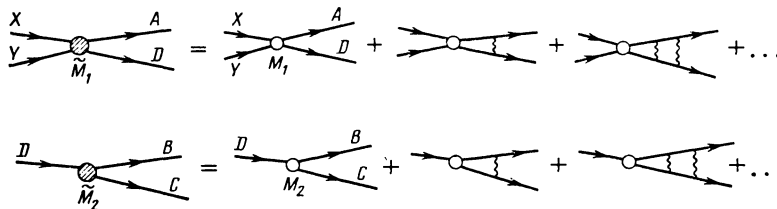


FIG. 2. Calculation of matrix elements \tilde{M}_1 , \tilde{M}_2 for treating the $A-D$ and $B-C$ interactions exactly.

for the amplitude. Here \tilde{M}_1 denotes the matrix element for the collision $X + Y \rightarrow A + D$, in which the $A-D$ Coulomb interaction is treated exactly; the matrix element \tilde{M}_2 for the decay $D \rightarrow B + C$ treats the $B-C$ interaction exactly (Fig. 2). This is important because the $A-D$ and $B-C$ interactions are strong at small distances. The potential $U(t, \tau)$ in (14) is equal to

$$U(t, \tau) = Z_A Z_B / |\mathbf{V}_{AD} t + \mathbf{V}_{AB} \tau| + Z_A Z_C / |\mathbf{V}_{AD} t + \mathbf{V}_{AC} \tau| - Z_A Z_D / |\mathbf{V}_{AD}(t + \tau)|. \quad (15)$$

The three terms in (15) are respectively the potential energies for the $A-B$, $A-C$, and $A-D$ interactions in the final state. The third term has a minus sign for the simple reason that particle D is not present in the final state; the interaction with D , which is included in the matrix element \tilde{M}_1 , must therefore be subtracted out in the final state. The interaction $B-C$ does not appear in $U(t, \tau)$ because it is already included in \tilde{M}_2 .

The term $\int U(t, \tau) d\tau$ in (14) has a simple physical interpretation—it is the classical action computed for straight-line trajectories. This term is responsible for the interaction in the final state (without it, (14) give the ordinary Breit-Wigner amplitude).

We note that the integral over τ in (12) and (14) is formally divergent at the upper limit because of the long-range nature of the Coulomb interaction. The standard procedure¹⁶ for avoiding this divergence is to cut off the potential at a distance $D \gg R$, where R is the characteristic radius R of the problem (5), and then let $D \rightarrow \infty$ in the resulting cross section. The upper limit T in the τ -integral in (14) is then finite ($T \gg R / V_A$), and T affects only the argument of the amplitude, not the cross section.

To find the cross section we must calculate $|A|^2$ [Eq. (14)] by substituting the explicit expression (15) for the potential $U(t, \tau)$. We consider a collision process (1) for which the velocities V_A , V_B , and V_C of the outgoing particles are specified. Energy and momentum conservation then implies that the cross section is determined by a five-dimensional set of independent parameters (e.g., the energy and scattering angle E_A , Ω_A of particle A and the scattering angle Ω_B of particle B). A straightforward calculation gives the following expression for the cross section:

$$\frac{d\sigma}{dE_A d\Omega_A d\Omega_B} = \sigma_0 \frac{\Gamma_{BC}}{2\pi(\varepsilon^2 + \Gamma^2/4)} k(\varepsilon), \quad (16)$$

$$k(\varepsilon) = \frac{\pi \xi}{\text{sh}(\pi \xi)} \exp\left(2\xi \arctg \frac{2\varepsilon}{\Gamma}\right). \quad (17)$$

Here Γ_{BC} is the partial width of the decay $D \rightarrow B + C$; it depends on the matrix element \tilde{M}_2 , while the cross section σ_0 for the collision $X + Y \rightarrow A + D$ depends on \tilde{M}_1 . The parameter ξ in (17) depends on the velocities of the particles emerging from the final state:

$$\xi = Z_A(Z_B/V_{AB} + Z_C/V_{AC} - Z_D/V_{AD}). \quad (18)$$

The three terms in (18) correspond to the three terms in the potential energy (15).

4. DISCUSSION

To analyze expression (16) for the cross section, we note that the first two factors describe an ordinary Breit-Wigner resonance. The factor $k(\varepsilon)$ (the principal result of this paper) describes the interaction of the particles in the final state. It depends on ε through the ratio Γ/ε and thus varies greatly over the linewidth, so that the Lorentzian line is appreciably distorted. A straightforward analysis of (16) reveals the following distortions:

1. The peak is shifted by $\Delta\varepsilon$,

$$\Delta\varepsilon = \xi\Gamma/2. \quad (19)$$

2. The peak intensity decreases monotonically as $|\xi|$ increases,

$$\left(\frac{d\sigma}{dE_A d\Omega_A d\Omega_B} \right)_{\max} = \frac{2\sigma_0\Gamma_{BC}}{\Gamma^2} \frac{\xi}{(1+\xi^2)\text{sh}(\pi\xi)} \exp(2\xi \text{arctg } \xi). \quad (20)$$

For large $|\xi| \gg 1$, the function (20) decays as $|\xi|^{-1}$, so that the line broadens in such a way that the total intensity remains constant. The line width $\tilde{\Gamma}$ at half-maximum is proportional to $|\xi|$ for large $|\xi|$:

$$\tilde{\Gamma} = \text{const } |\xi|. \quad (21)$$

3. The line becomes asymmetric. (These assertions are illustrated in Fig. 5, which is discussed below.)

All these spectral changes depend only on the single parameter ξ (18). According to (16) and (17), the distortion increases with $|\xi|$. It is important to note that our underlying assumptions (5)–(7) do not rule out the possibility that one or all of V_{AD} , V_{AB} , V_{AC} may be small (< 1). It is therefore possible for $|\xi|$ to exceed unity, so that the spectral distortions may be significant.

We now apply these results to the reactions (2)–(4), where A is an ion or electron, B is an autoionizing electron, and D and C are heavy atomic particles, so that $V_D \approx V_C \approx 0$. Expression (18) for ξ then simplifies to

$$\xi = -Z_A Z_B (V_A^{-1} - V_{AB}^{-1}). \quad (22)$$

If we assume that the autoionizing electron is fast ($V_B \gg V_A$), then ξ (22) [and hence also the cross section (16)] is independent of Ω_A ; this case has been analyzed extensively in the literature.¹⁻⁹ The shift $\Delta\varepsilon$ (19) is then given by the familiar Barker-Berry formula,¹ which in our situation takes the form

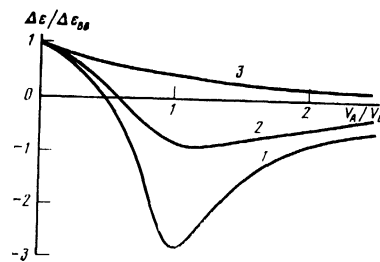


FIG. 3. Dependence of the energy shift calculated by (19), (22) as a function of the velocity ratio and angle θ between the outgoing particles. 1) $\theta = 15^\circ$; 2) $\theta = 30^\circ$; 3) $\theta = 120^\circ$. The energy shift is normalized by the Barker-Berry shift (23).

$$\Delta\varepsilon_{BB} = -\Gamma Z_A Z_B / 2V_A. \quad (23)$$

$\Delta\varepsilon_{BB}$ is also independent of Ω_A and Ω_B , and it does not change sign as V_A varies.

The situation is completely different if $V_A \sim V_B$; in this case ξ given by (22) is sensitive to the angle θ between A and B ($\cos \theta = V_A V_B / V_A V_B$), and even the sign of ξ depends on θ . This is illustrated in Fig. 3, which plots $\Delta\varepsilon$ (19) as a function of V_A/V_B and θ . We see that the shift is sensitive to θ when $V_A = V_B$ but independent of θ in the limit $V_A \ll V_B$.

Let us now discuss how the above results might be verified experimentally. For reactions (3) and (4) there are two electrons in the final state. Complicated coincidence experiments are necessary to measure their velocities, on which $k(\varepsilon)$ (16) depends. Although such experiments have not been carried out, much experimental work has been done for the case when only a single autoionizing electron is present.

To describe these experimental results we must integrate the cross section (16) over Ω_A , the scattering angles for particle A on which both $k(\varepsilon)$ and σ_0 depend. Since the dependence $\sigma_0(\Omega_A)$ is not known *a priori*, we will use two very simple models to perform an average.

To a very rough approximation, the experimental shift of the spectral line for particle B is given by

$$\overline{\Delta\varepsilon} = \frac{1}{4\pi} \int \Delta\varepsilon d\Omega_A = \Delta\varepsilon_{BB} \begin{cases} 1 - V_A/V_B, & V_B \geq V_A \\ 0, & V_B \leq V_A \end{cases} \quad (24)$$

with $\Delta\varepsilon$ and $\Delta\varepsilon_{BB}$ defined by (19) and (23). The approximation on the right in (24) was first suggested in Ref. 10 and was subsequently demonstrated numerically.¹¹

A more accurate estimate for $\Delta\varepsilon$ can be obtained by averaging the cross section (16) over Ω_A and taking σ_0 to be isotropic. We carried out such a calculation numerically for electron impact excitation of the $2s^2(^1S_0)$ and $2s^{-1}3s(^1S)$ autoionizing states in helium and neon, respectively. Figure 4 shows how the shift $\Delta\varepsilon(\bar{\sigma})$ in the maximum of the cross section averaged in this way depends on the amount ΔE by which the energy of the incident electron exceeds the excitation threshold. The figure also plots $\overline{\Delta\varepsilon}$ (24) and $\Delta\varepsilon_{BB}$ (23) along with available experimental data. In spite of the crudeness of the assumptions used to average the cross section, the results agree fairly well with the experimental findings (the agreement is considerably closer than for the Barker-Berry model¹). We note that both our calculations and the experimental results imply that the sign of the shift is constant.

It would be of great interest to experimentally verify the

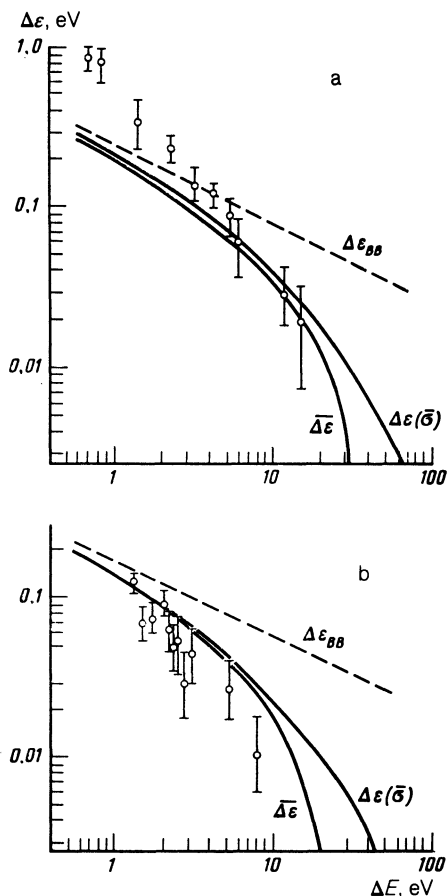


FIG. 4. Energy shift of the spectral line for autoionizing electrons as a function of the energy excess ΔE of the incident electron above the excitation threshold (the atoms were excited by electron impact); $\overline{\Delta\epsilon}$ and $\Delta\epsilon(\overline{\theta})$ are defined in the text. a) $2s^{-1}S_0$ autoionization spectrum for He, $\Gamma = 138$ meV; experimental data from Ref. 18; b) $2s^{-1}S_1$ autoionization spectrum for Ne, $\Gamma = 95$ meV; experimental data from Ref. 19.

change in sign of the shift $\Delta\epsilon$ predicted by Eqs. (19) and (22); this would probably be easiest for ion-atom collisions (2). For ion velocities that are not too small ($V_I \sim 1$), there is a high probability that the ion trajectory will be almost straight. It thus suffices to measure the spectrum of the electrons when the outgoing electron makes various angles θ relative to the incident beam. The above theory predicts that the spectral changes should be sensitive to θ . This is illustrated in Fig. 5, which shows the electron spectrum calculated by Eq. (16) for excitation of the neon $2s^{-1}3s^1(^1S_0)$ autoionizing state by 40.3 keV incident protons (this energy was chosen so that the proton velocity was equal to the velocity of the outgoing electron). We see that the position and shape of the line are sensitive to θ . This result has a simple physical interpretation—the repulsion between the proton and the ion is most important for large θ and causes the proton ener-

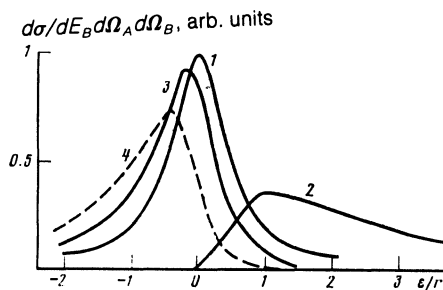


FIG. 5. Calculated electron spectra (16) near the $2s^{-1}3s(^1S_0)$ autoionizing state in Ne (excited by proton impact). 1) neglecting the interaction in the final state; 2, 3) predictions of Eq. (16) for several angles between the incident proton and outgoing electron: 2) $\theta = 15^\circ$; 3) $\theta = 120^\circ$; 4) neglecting the proton-electron interaction (Barker-Berry approximation).

gy to increase; for small θ , the proton-electron attraction is more important, and the proton loses energy.

We note that our theory is invalid for very large θ because conditions (7) are violated. In this case, the cross section is also sensitive to coherent processes involving the direct ionization atoms by protons, and in particular to charge transfer into the continuous spectrum.¹⁷

In closing, it is a pleasant duty to thank M. Ya. Amus'ya and G. N. Ogurtsov for helpful discussions of the above results.

¹R. B. Barker and H. W. Berry, Phys. Rev. **151**, 14 (1966).

²G. C. M. King, F. H. Read, and R. C. Bradford, J. Phys. B **8**, 2210 (1975).

³F. H. Read, Radiat. Res. **64**, 23 (1975).

⁴A. Niehaus, J. Phys. B **10**, 1845 (1977).

⁵V. N. Ostrovskii, Zh. Eksp. Teor. Fiz. **72**, 2079 (1977) [Sov. Phys. JETP **45**, 1092 (1977)].

⁶M. Ya. Amusia, M. Yu. Kuchiev, S. A. Sheinerman, and S. I. Sheftel, J. Phys. B **10**, L535 (1977).

⁷M. Ya. Amus'ya, M. Yu. Kuchiev, and S. A. Sheinerman, Zh. Eksp. Teor. Fiz. **76**, 470 (1979) [Sov. Phys. JETP **49**, 238 (1979)].

⁸M. Yu. Kuchiev and S. A. Sheinerman, J. Phys. B **18**, L551 (1985).

⁹K. Helenelund, S. Hedman, L. Asplund, U. Gelius, and K. Siegbahn, Phys. Scripta **27**, 245 (1983).

¹⁰G. N. Ogurtsov, J. Phys. B **16**, L745 (1983).

¹¹J. Mizuno, T. Ishihara, and T. Watanabe, J. Phys. B **18**, 1241 (1985).

¹²A. I. Baz', Ya. B. Zel'dovich, and A. M. Perelomov, *Scattering, Reactions, and Decay in Nonrelativistic Quantum Mechanics*, Wiley, New York (1969).

¹³M. Ya. Amusia and M. Yu. Kuchiev, Phys. Rev. Lett. **48**, 1726 (1982).

¹⁴M. Yu. Kuchiev, J. Phys. B **18**, L579 (1985).

¹⁵J. E. Brown and A. D. Jackson, *The Nucleon-Nucleon Interaction* North-Holland, Amsterdam (1976).

¹⁶V. B. Berestetskii, E. M. Lifshitz, and L. P. Pitaevskii, *Kvantovaya Elektrodinamika (Quantum Electrodynamics)*, Nauka, Moscow (1980); Engl. Transl. Oxford (1982).

¹⁷V. N. Mileev, V. S. Senashenko, and E. Yu. Tsymbal, in: Proc. 2nd Sci. Sem. on Autoionization Phenomena in Atoms, MGU (1981), p. 79.

¹⁸A. J. Smith, P. J. Hicks, F. H. Read, S. Cvejanovic, G. C. King, J. Comer, and I. M. Sharp, J. Phys. B **7**, L496 (1974).

¹⁹D. G. Wilden, P. J. Hicks, and J. Comer, J. Phys. B **10**, 1477 (1977).

Translated by A. Mason